Effect of dye concentrations in blended-layer white organic light-emitting devices based on phosphorescent dyes

C. Pearson,[1] D. H. Cadd,[1] M. C. Petty,[1,a)] and Y. L. Hua[2]
[1]*School of Engineering and Centre for Molecular and Nanoscale Electronics, Durham University, Durham DH1 3LE, United Kingdom*
[2]*Institute of Material Physics, Tianjin University of Technology, Tianjin 300191, People's Republic of China*

(Received 9 June 2009; accepted 18 August 2009; published online 30 September 2009)

The electronic and optoelectronic behavior of white organic light-emitting devices (OLEDs) based on blue (FIrpic) and red [$Ir(piq)_2(acac)$] phosphorescent dyes doped into the same layer of a polyvinylcarbazole (PVK) host are reported. The conductivity of all the OLEDs studied appeared to be dominated by space-charge injection effects, exhibiting a current I versus voltage V dependence of the form $I \propto V^n$, with $n \approx 7$ at applied voltages at which electroluminescence was observed. Systematic studies of the current versus voltage and light-emitting behavior of the OLEDs have identified different excitation processes for the two dyes. It is suggested that electroluminescence from the FIrpic molecules originates by direct transfer of the exciton energy from the PVK to the dye molecules, while the process of light emission from the $Ir(piq)_2(acac)$ molecules involves carrier trapping. The efficiency of the devices can be tuned, to some extent, by varying the thickness of the organic film. Luminous efficiencies and luminous power efficiencies of 8 cd A^{-1} and 3 lm W^{-1} were measured for these blended-layer OLEDs, with Commission Internationale de l'Eclairage coordinates of 0.35, 0.35. © *2009 American Institute of Physics*.
[doi:10.1063/1.3226780]

I. INTRODUCTION

Electroluminescence (EL) in organic materials is now the subject of intense worldwide research.[1] Many compounds, both molecular and polymeric, have been developed for use in organic light-emitting devices (OLEDs) for display applications. Red, green, and blue (RGB) emission is necessary to make full color displays. In addition to the three primaries, white has been considered to be important as color images can be realized by combining the white emission with RGB filters. Furthermore, there is a growing research activity focused on the exploitation of white OLEDs for solid-state lighting applications. To produce white emission, the three primary colors or two complementary colors must be combined. If properly chosen, it is easier to adjust the composition of a two-component system. The various strategies that have been used have been reviewed in the literature.[2,3]

Many OLEDs exploit organotransition metal compounds consisting of triplet emitters.[4] The internal quantum efficiencies of devices based on these compounds may be a factor of 4 higher than for purely organic emitter materials, leading to white OLEDs with efficiencies comparable to fluorescent tubes.[5] This results from phosphorescent emission from the lowest excited electronic triplet state to the singlet ground state. Although this transition is normally forbidden, it may become sufficiently allowed by spin-orbit coupling induced by the central metal ion (e.g., Ir or Ru). Different physical mechanisms of electron-hole recombination (exciton formation and population of the emitting triplet state) can occur. For example, the exciton can be formed and trapped on the host molecule with subsequent energy transfer to the triplet emitter. In an alternative process, one of the charge carriers is directly trapped on the emitter dopant itself and the recombination occurs on this molecule. Energy transfers from host donors to guest acceptors may occur by Förster and/or Dexter mechanisms. The former involves relatively long-range (up to ~10 nm), nonradiative, dipole-dipole coupling of the donor and acceptor molecules. This requires a significant overlap of the emission of the host and the adsorption of the guest. On the other hand, Dexter energy transfer is a short-range (typically ~1 nm) process in which excitons diffuse from donor to acceptor sites via intermolecular electron exchange. Efficient Dexter transfer requires an overlap of the host and guest wave functions and that the energy of the (singlet and triplet) exciton on the host matches the exciton energy of the guest.

Here, we report on the electronic and optoelectronic behavior of white OLEDs based on the phosphorescent emitters bis[(4,6-difluorophenyl)-pyridinato-N, $C^{2'}$] (picolinato) Ir(III); FIrpic, a blue emitter; and bis(1-phenylisoquinoline) (acetylacetonate) Ir(III) [$Ir(piq)_2(acac)$], a red emitter. These dyes are doped into a matrix consisting of a polyvinylcarbazole (PVK) host and an electron transport compound 1,3-bis[(4-tert-butylphenyl-1,3,4-oxadiazolyl) phenylene (OXD7). In such a blended OLED structure, the emitting layer is formed from a single spin-coated layer. Devices should therefore be easy to fabricate.[6,7] Furthermore, the relative positions of the emissions from the FIrpic[8] and $Ir(piq)_2(acac)$[9] on the Commission Internationale de l'Eclairage (CIE) chromaticity diagram indicate that white emission should be possible using a device structure that incorporates only two emissive components, again simplifying manufacture.

a)Electronic mail: m.c.petty@durham.ac.uk.

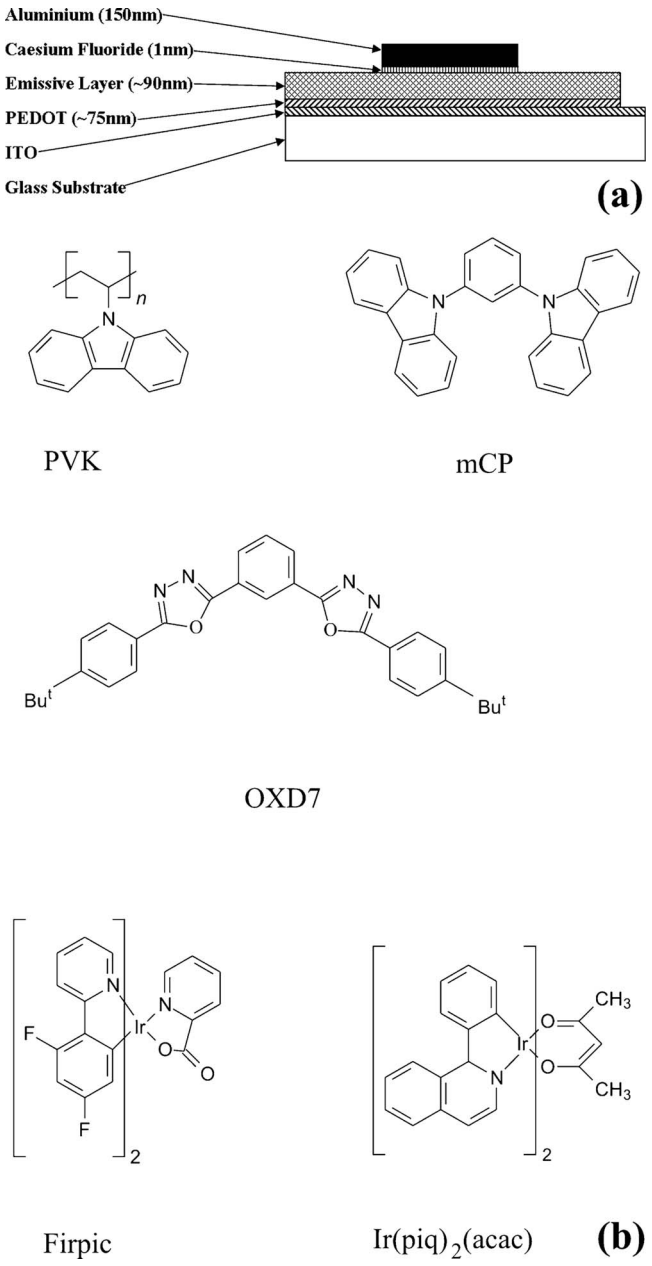

FIG. 1. (a) Schematic diagram depicting the OLED configuration used in this work. (b) Chemical structure of organic molecules used in this work.

II. EXPERIMENT

Figure 1(a) shows a schematic diagram of the device structure used in this investigation. Devices were fabricated on indium tin oxide (ITO) coated glass supplied by Merck (Germany). The sputtered ITO layer, which formed the anode of the device, was 200-nm-thick with a sheet resistance of 8 Ω/sq.

The substrates were cut to size ($\sim 16 \times 21$ mm) before being carefully cleaned using the following procedure: rinsed in a jet of isopropyl alcohol (IPA) (laboratory reagent grade, Fisher Scientific) from a wash bottle; sonicated in IPA for 15 min; rinsed in a jet of IPA from a wash bottle; dried in a stream of nitrogen gas; rinsed in a jet of acetone (analytical reagent grade, Fisher Scientific) from a wash bottle; sonicated in acetone for 15 min; rinsed in a jet of acetone from a wash bottle; dried in a stream of nitrogen gas; rinsed in a stream of ultrapure water (obtained by reverse osmosis, carbon filtration, two stage de-ionization, and UV sterilization); sonicated in a solution of Decon 90 detergent (5% in ultrapure water) for 15 min; rinsed in a stream of ultrapure water; sonicated in ultrapure water for 15 min; rinsed in a stream of ultrapure water; and finally dried in a stream of nitrogen gas.

Device fabrication was performed in an inert gas glove box (Glove Box Technology Ltd.). Cleaned substrates were first spin-coated with an ~75-nm-thick layer of poly(3,4-ethylenedioxythiophene)/poly(styrenesulfonate) (PEDOT/PSS) from aqueous dispersion (CLEVIOS P VP AI 4083, H. C. Starck, Germany). Before coating, the PEDOT/PSS solution was passed through a 0.2 μm syringe filter to remove any residual particulates. 200 μl of the filtered dispersion was applied to the surface of the substrate, which was then spun at 2500 rpm for 45 s. The coated substrates were annealed at 180 °C for 2 min to remove any residual water.

The chemical structures of the various materials that were used to form the blended electroluminescent layer in these devices are shown in Fig. 1(b): PVK (average M_W ~1 100 000, Aldrich); 3, 5′-*N*, *N*′-dicarbazole-benzene (mCP); OXD7; FIrpic; and $Ir(piq)_2(acac)$ (Luminescence Technology Corp.). All compounds were used as-supplied, without further purification. Separate chlorobenzene (AnalaR, BDH) solutions of each material were prepared before mixing in the proportions necessary to give a blended solution of the required concentration and composition. The concentrations expressed as percentages throughout this paper are all by weight percent. 150 μl of this solution was applied to the surface of the substrate, which was then spun for 60 s at the speed necessary to give a layer having the desired thickness. The coated substrates were annealed at 80 °C for 30 min to remove any residual chlorobenzene solvent.

The final fabrication step was the deposition of a 2×3 array of 5 mm diameter cesium fluoride (CsF, 99.99%, Aldrich)/aluminum (Al, AnalaR, BDH) cathodes by thermal evaporation through a shadow mask. The deposition was carried out under a base vacuum of $\sim 4 \times 10^{-6}$ mbar ($\sim 3 \times 10^{-6}$ torr). Approximately 1 nm of CsF was deposited at a rate of 0.20 ± 0.05 nm s^{-1}, followed by ~150 nm of Al at a rate of 1.0 ± 0.1 nm s^{-1}.

Electrical measurements were carried out under vacuum ($\sim 10^{-1}$ mbar) in a screened metal chamber. Bias voltages were supplied and sample currents measured using a Keithley model 2400 sourcemeter. The devices were mounted over a large area photodiode and the photocurrent generated as a result of the light output was recorded using a Keithley model 485 digital picoammeter. The instruments were connected via general purpose interface bus (GPIB) to a personal computer, which was used to automate the measurement process.

Photometric and colorimetric measurements were performed using a Photo Research Inc. PR-655 SpectraScan spectroradiometer fitted with a FP-655 flexible probe (3.18 mm tip diameter).

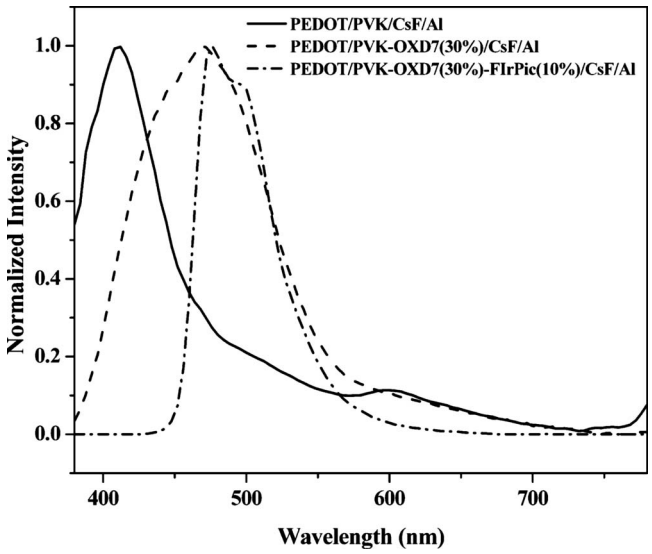

FIG. 2. Normalized EL spectra of OLEDs with the configurations: ITO/PEDOT/PVK/CsF/Al (full line); ITO/PEDOT/PVK-OXD7(30%)/CsF/Al (dashed line); and ITO/PEDOT/PVK-OXD7(30%)-FIrpic(10%)/CsF/Al (dashed-dotted line).

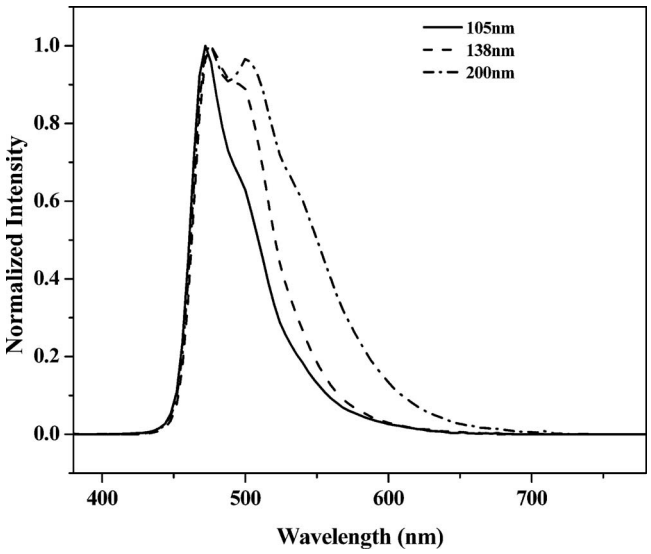

FIG. 3. Normalized EL spectra for ITO/PEDOT/PVK-OXD7(30%)-FIrpic(10%)/CsF/Al OLEDs with different organic layer thicknesses: full line, 105 nm; dashed line, 138 nm; dashed-dotted line, 200 nm.

III. RESULTS AND DISCUSSION

A. Blue device operation

Figure 2 contrasts the normalized EL spectra of three devices measured at a current of 1 mA (current density 5.1 mA cm^{-2}): (i) ITO/PEDOT/PVK/CsF/Al; (ii) ITO/PEDOT/PVK-OXD7 (30%) /CsF/Al; and (iii) ITO/PEDOT/PVK-OXD7 (30%)-FIrpic(10%)/CsF/Al. The PVK emission is a maximum at 415 nm, with an additional peak at about 600 nm. The emission at the longer wavelength has been attributed to triplet excimers in the PVK.[10] The addition of the OXD7 results in a much broader EL spectrum centered around 470 nm, which may be related to exciplex formation (i.e., the coupling of an excited singlet state of one molecule with the ground state of another). The emission for mixtures of PVK with the similar hole transport compound 2-(4-biphenylyl)-5-(4-tert-butylphenyl)-1,3,4-oxadiazole (PBD) has previously been assigned to an exciplex formed between a hole on PVK and an electron on PBD.[11] The addition of FIrpic to our PVK-OXD7 device results in blue emission, with a maximum in the EL spectrum at 480 nm together with a shoulder at about 505 nm. This emission is similar to that reported previously for FIrpic doped into PVK,[3,12] and is also characteristic of the emission observed when FIrpic is mixed in other host matrices, e.g., 4, 4′-bis(9-carbozolyl)-2, 2′-biphenyl (CBP),[13] 4, 4′-bis(9-carbazolyl)-2, 2′-dimethyl-biphenyl (CDBP),[8] or mCP.[14] No PVK emission (either at 415 or 600 nm) is evident in the FIrpic-containing OLED, suggesting good energy transfer between the host matrix and the guest dye.

The relative intensities of the FIrpic emission bands were found to be very dependent on the thickness of the blended layer. For example, Fig. 3 compares the EL spectra for three OLEDs spin-coated from different concentration blend solutions (10, 16, and 25 g l^{-1}); the total thicknesses of the organic layers in these devices were 105, 138, and 200 nm. Emission peaks at around 480 and 510 nm, together with a shoulder at about 540 nm, are evident. These almost certainly correspond to the 0–0, 0–1, and 0–2 bands in the triplet emission of FIrpic that are observed in the photoluminescence spectra (at 465.2, 495.6, and about 525 nm).[13] We attribute the change in intensity of the bands with film thickness to a microcavity effect, which favors the red emission for the thicker structures.[15,16]

The current I versus voltage V behavior for the OLEDs, the EL spectra of which are depicted in Fig. 2, are contrasted in Fig. 4(a). The ITO/PEDOT/PVK/CsF/Al device exhibits a relatively low conductivity. It is expected that the current carriers in this structure are mainly holes. Addition of the OXD7 electron transport compound increases the current significantly; the extra current carriers are likely to be electrons. For the OXD7 concentration used (30%), Fig. 4 shows that the incorporation of the electron transport compound has increased the current by more than a factor of 2 for an applied voltage of 10 V. This indicates that a good balance of hole current to electron current has been achieved. The addition of the 10% FIrpic does not affect the current through the OLED appreciably, suggesting that not much of the current passes through the dye molecules, which will be too far apart to facilitate carrier hopping. Section III C, later, describes the effect of different FIrpic concentrations on the optoelectronic behavior of the OLEDs.

Various electrical conductivity mechanisms have been reported to operate in OLEDs. These include Fowler–Nordheim tunneling through interface barriers,[17] space-charge limited conduction,[18,19] and Schottky barrier formation.[20,21] Such processes can be distinguished by studying the dependence of the current on the applied voltage. The I versus V characteristics shown in Fig. 4(a) are replotted in log-log format in Fig. 4(b). Over the voltage range used, the current voltage behavior is of the form $I \propto V^n$. At low bias, the PVK structure exhibits an n value between 1 and 2, whereas the devices containing additional OXD7 and OXD7+FIrpic show an almost linear dependence of current

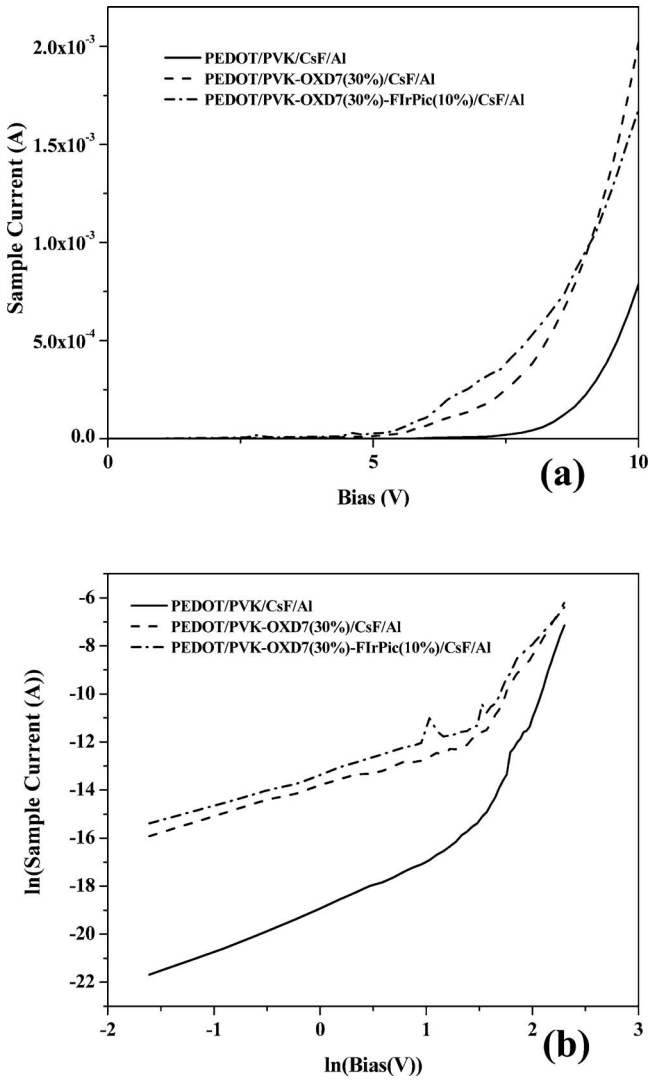

FIG. 4. (a) Current vs bias data for OLEDs with different configurations: ITO/PEDOT/PVK/CsF/Al (full line); ITO/PEDOT/PVK-OXD7(30%)/CsF/Al (dashed line); and ITO/PEDOT/PVK-OXD7(30%)-FIrpic(10%)/CsF/Al (dashed-dotted line). (b) Same data plotted in ln I vs ln V format.

on applied voltage. For applied voltages greater than about 5 V, corresponding to the point where EL can be detected, the n values are much larger for all the devices studied—approximately 12 for the control PVK device and about 7 for the other two OLEDs.

The above data suggest that the conductivity of our devices is limited by space-charge effects in the organic layers. Campbell and co-workers[18,19] have shown that a model involving space-charge limited conductivity with an exponential distribution of traps provides an excellent agreement with the experimentally observed current versus voltage data for poly(phenylene vinylene) (PPV) OLEDs. In this case, the current density J versus voltage relationship takes the form[18]

$$J = K\frac{V^{m+1}}{d^{2m+1}}, \tag{1}$$

where K is a constant related to the highest occupied molecular orbital (HOMO) effective density of states and carrier mobility, d is the thickness of the organic layer, and m is a constant related to the characteristic energy E_t of the exponential trap energy distribution by

$$m = \frac{E_t}{kT}. \tag{2}$$

$m \to \infty$ implies a uniform distribution of traps in energy, while $m=1$ suggests shallow traps, as predicted by the simple space-charge limited conductivity model (i.e., Child's law).[22] Values of $m+1$ of about 7 were reported by Campbell *et al.*[18] for their PPV OLEDs operating in the high bias regime at 290 K, which is similar to the data shown in Fig. 4(b). However, the theory of Eq. (1) could not explain the observed thickness dependence of the electrical behavior of some of their OLEDs. Preliminary measurements on our samples revealed a similar problem. Based on the result $m+1=7$ for the FIrpic OLED in the high bias regime [Fig. 4(b)], we would anticipate a current density dependence on film thickness (constant applied bias) of $J \propto d^{-13}$ from Eq. (1). However, an initial study of the current dependence on thickness for our PVK-OXD7(30%)-FIrpic(10%) OLEDs revealed $J \propto d^{-4}$ in the high bias regime. Campbell *et al.*[18] suggested that mixed models in which the field-dependent (Poole–Frenkel) detrapping occurs from the exponential trap distribution, or in which carriers have the hopping transport mobility, but are also trapped by the exponential trap distribution, might provide an improvement over Eq. (1). However, further details of the carrier mobilities and the nature of the traps would be required to distinguish between these models.

The current versus voltage behavior at lower biases was also discussed by Campbell *et al.*[18] and attributed to pure space-charge limited current flow (i.e., Child's law, no traps). In our case, it is plausible that this is the situation for the PVK device. However, the significantly higher currents noted in both the PVK-OXD7 and PVK-OXD7-FIrpic OLEDs, together with the almost linear current versus voltage behavior noted below 5 V suggest that simple Ohmic conductivity may dominate at these low voltages for these particular devices. In these cases, the number of injected carriers is negligible compared to those already available in the material.

The luminous efficiency and the luminous power efficiency of our blue FIrpic-doped OLED were about 20 cd A^{-1} and 9 lm W^{-1}, respectively, measured at a current of 1 mA (applied voltage=7 V). The corresponding brightness was about 1000 cd m^{-2}; this increased to about 5000 cd m^{-2} for a current of 5 mA.

During the course of this work, approximately 250 batches of samples were manufactured, in groups of six OLEDs. This provided an opportunity to study the variations in the electrical parameters within batches and between batches of OLEDs, which had been manufactured ostensibly under identical conditions. The deviations in the luminous efficiencies and the luminous power efficiencies for devices within the same batch were approximately $\pm 4\%$. In contrast, a larger variation of about $\pm 13\%$ was found in the efficiencies of OLEDs between batches [19 sets of the reference ITO/PEDOT/PVK-OXD7 (30%)-FIrpic(10%)/CsF/Al structures were made during our investigations]. Within these ex-

TABLE I. Efficiency data for ITO/PEDOT/Host-OXD7-FIrpic(10%)/CsF/Al OLEDs, in which the host material was either PVK or mCP.

Host	OXD7	Device voltage at 1 mA(V)	Brightness at 1 mA (cd m^{-2})	Luminous efficiency at 1 mA(cd A^{-1})	Luminous power efficiency at 1 mA(lm W^{-1})	External quantum efficiency at 8 mA(%)
PVK	30%	7	1000	20	9.0	5.3
mCP	30%	6.3	184	3.6	1.8	1.5
mCP	0%	6.3	103	2.7×10^{-2}	1.3×10^{-2}	0.1

perimental errors, our efficiency data are in line with those reported by other groups for FIrpic-based OLEDs. For example, Lee *et al.*[23] provide figures of around 20 cd A^{-1} and 5–10 lm W^{-1} for the luminous efficiency and the luminous power efficiency, respectively, of FIrpic devices incorporating a variety of hole and electron-transporting compounds and using mCP as the host matrix. Similar efficiency data are reported by Tokito *et al.*[8] using CDBP as the host and for devices incorporating a hole transporting layer adjacent to the PEDOT/PSS layer [4, 4′-bis[*N*-(1-naphthyl)-*N*-phenyl-amino]biphenyl] and an electron-transporting/hole-blocking layer [aluminum (III) bis(2-methyl-8 quinolinato)4-phenylphenolate] beneath the cathode. A FIrpic-OXD7-doped PVK structure, reported by Krummacher *et al.*,[3] possessed a luminous current efficiency of about 20 cd A^{-1} at a brightness of 1000 cd m^{-2}.

The triplet energy of FIrpic is 2.6–2.7 eV,[4,8,24] greater than the reported figure of 2.5 eV for PVK.[4] This situation could result in some of the triplet energy on the FIrpic molecules being transferred to the PVK and subsequently lost through nonradiative decay. We have therefore experimented using mCP as a host for the FIrpic dye; mCP is reported to possess high triplet energy (2.9 eV) and a high photoluminescence efficiency.[25] However, the results, summarized in Table I, reveal a significantly poorer OLED performance for mCP-based devices. This suggests that the PVK may well possess a higher triplet energy than the 2.5 eV noted above. Values up to 3.0 eV have been reported in the literature.[26,27]

The lowest unoccupied molecular orbital levels of OXD7 and FIrpic are similar [−2.9 eV for FIrpic (Ref. 23) and −2.8 eV for OXD7 (Ref. 25)]. The phosphorescent dye molecules are therefore not likely to act as electron traps. Similarly, hole trapping by the FIrpic is unlikely as the HOMO level of the latter [(−5.8 eV) (Ref. 23)] is below that of PVK (−5.6 eV).[4] This is consistent with the fact that the addition of FIrpic does not seem to affect the device current appreciably (Fig. 4). We therefore suggest that the blue emission from our OLEDs results from the transfer of excitons formed on the PVK molecules directly to the FIrpic.

For completeness, we have studied the influence of the layers adjacent to the metal anode and cathode on the properties of our reference blue OLEDs (the effect of varying the OXD7 concentration is discussed in the following section). FIrpic-based devices with no PEDOT layer [i.e., ITO/PVK-OXD7(30%)-FIrpic(10%)/CsF/Al] were found to possess efficiencies that were reduced by at least three orders of magnitude, indicating the importance of this hole transport layer in our OLEDs. The effect of varying the thickness of the CsF layer was less marked. The introduction of a CsF layer, 1–7 nm in thickness, was found to increase both the luminous and luminous power efficiencies by a factor of around 2.

B. Effect of red dye concentration

The effect of adding various concentrations of $Ir(piq)_2(acac)$ to the blue OLED described in the previous section is shown in Fig. 5. As the red dye content in the blended-layer film is increased, a new emission band above 600 nm becomes evident. At a 5% $Ir(piq)_2(acac)$ concentration, the FIrpic emission is effectively zero. The corresponding changes in the CIE diagram are depicted in Fig. 6. The

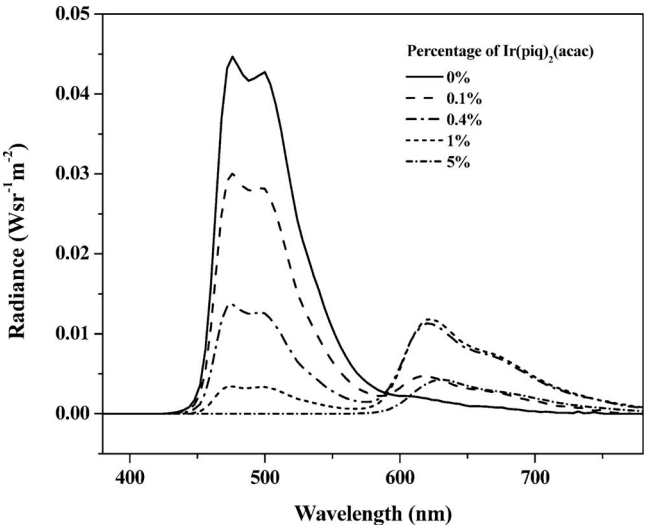

FIG. 5. EL spectra of ITO/PEDOT/PVK-OXD7(30%)-FIrpic(10%)-$Ir(piq)_2(acac)(x\%)$/CsF/Al with different x (by weight) values.

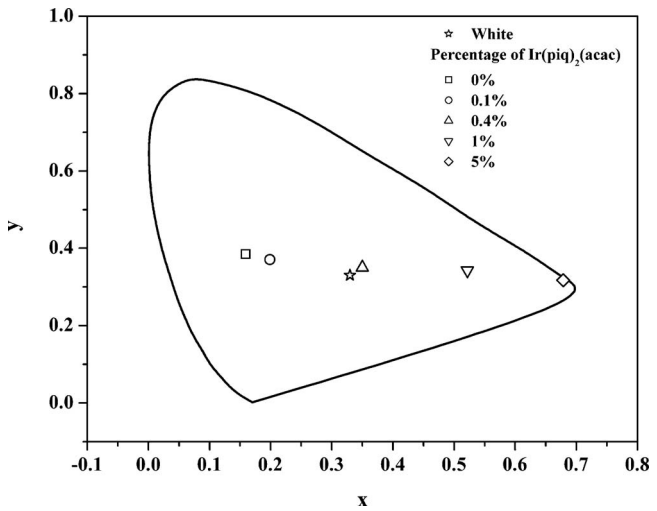

FIG. 6. CIE coordinates for OLEDs, the EL spectra of which have been shown in Fig. 5.

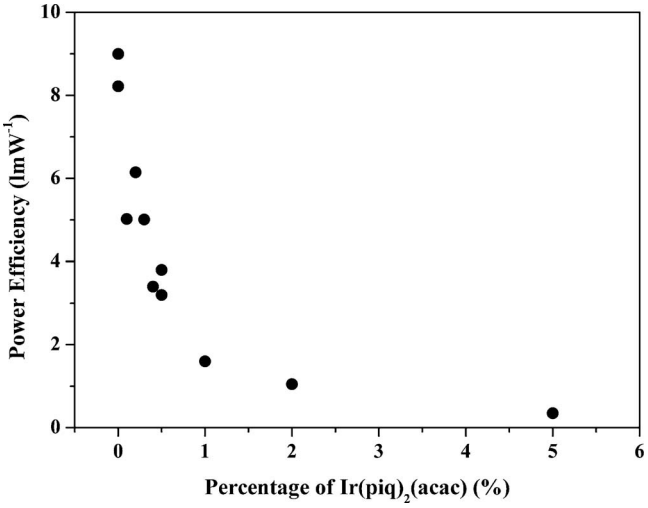

FIG. 7. Luminous power efficiency vs concentration (x%) of Ir(piq)$_2$(acac) for OLEDs with the configuration ITO/PEDOT/PVK-OXD7(30%)-FIrpic(10%)-Ir(piq)$_2$(acac)(x%)/CsF/Al.

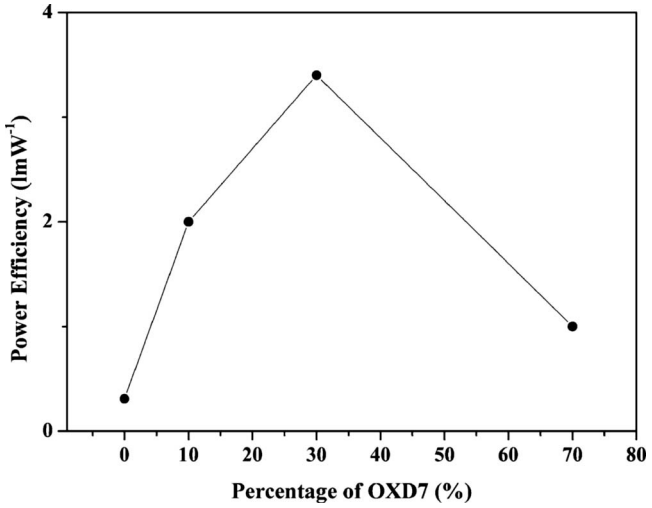

FIG. 8. Luminous power efficiency vs OXD7 concentration, measured at a current of 0.5 mA, for OLEDs with configuration ITO/PEDOT/PVK-OXD7 (x%)-FIrpic(10%)-Ir(piq)$_2$(acac)(0.4%)/CsF/Al.

locus of the data points passes very close to pure white (0.33, 0.33), with an optimum red dye concentration of 0.4% for the best white device (0.35, 0.35). The current and power efficiencies of this device at a drive current of 1 mA (applied voltage=7.3 V) were 7.8 cd A^{-1} and 3.4 lm W^{-1}, respectively, and the corresponding brightness was about 400 cd m^{-2}. The efficiencies of the blended-layer OLEDs decreased markedly with an increase in Ir(piq)$_2$(acac), as shown in Fig. 7 for the case of the power efficiency.

The 30% OXD7 concentration was found to be the optimum in our experiments. Figure 8 shows the power conversion efficiency of a ITO/PEDOT/PVK-OXD7-FIrpic(10%)-Ir(piq)$_2$(acac)(0.4%)/CsF/Al for different OXD7 concentrations; the luminous power efficiency clearly peaks at a concentration of the electron transport compound of around 30%. This suggests that this composition results in a good balance of electron and hole currents in the OLED.

The current versus voltage behavior of ITO/PEDOT/PVK-OXD7(30%)-FIrpic (10%)-Ir(piq)$_2$(acac)(x%)/CsF/Al OLEDs in which x varied from 0 to 5 is shown in Fig. 9: Fig. 9(a), I versus V and Fig. 9(b), ln$I$ versus ln$V$. The curves reveal the same basic characteristics as shown in Fig. 4, i.e., at low bias the current is almost proportional to the voltage, whereas the high bias regime (>5 V) reveals a power law dependence of the form of Eq. (1). The value of $m+1$ is approximately 7 for all the red dye concentrations studied [i.e., similar to that noted in Fig. 4(b) for the PVK-OXD7 and PVK-OXD7-FIrpic devices], suggesting that the underlying conductivity mechanism is unaffected by the introduction of Ir(piq)$_2$(acac). However, it is apparent from Fig. 9 that the device current decreases as the red dye content is increased. The HOMO level of Ir(piq)$_2$(acac) has been calculated as −4.8 eV.[9] In contrast to the case for FIrpic, this lies within the band gap of the PVK. The addition of Ir(piq)$_2$(acac) molecules is therefore likely to lead to hole trapping, accounting for the reduction in the device current. This offers an additional route to the excitation of the Ir(piq)$_2$(acac). The increase in our device resistance with increasing red dye concentration leads to an increase in the

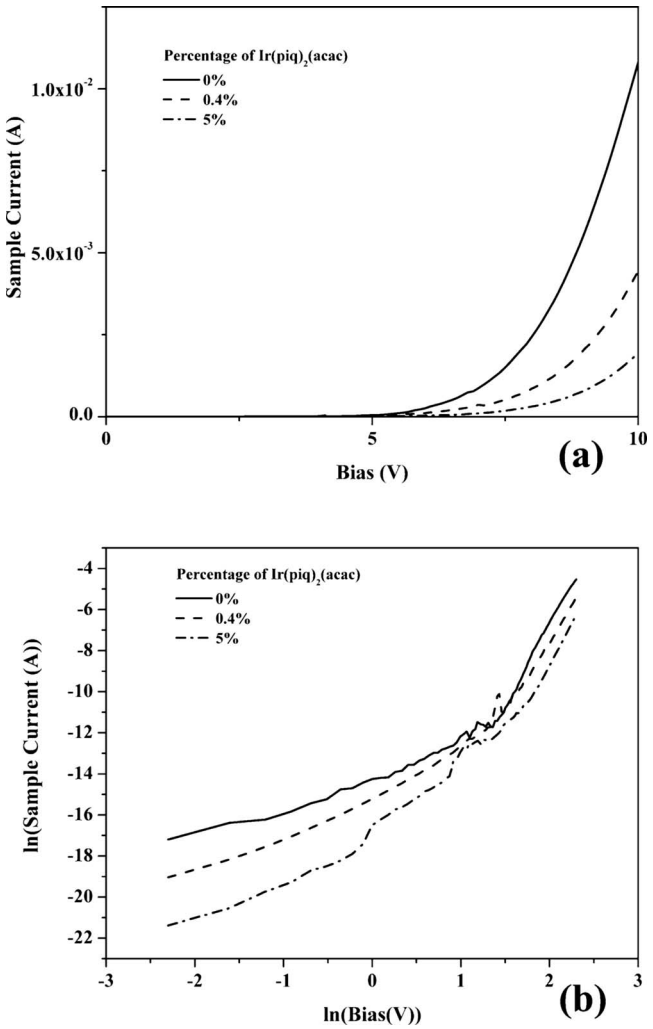

FIG. 9. (a) Current vs bias data for OLEDs with the configuration ITO/PEDOT/PVK-OXD7(30%)-FIrpic(10%)-Ir(piq)$_2$(acac)(x%)/CsF/Al: full line x=0; dashed line x=0.4; dashed-dotted line x=5. (b) Same data plotted in ln I vs ln V format.

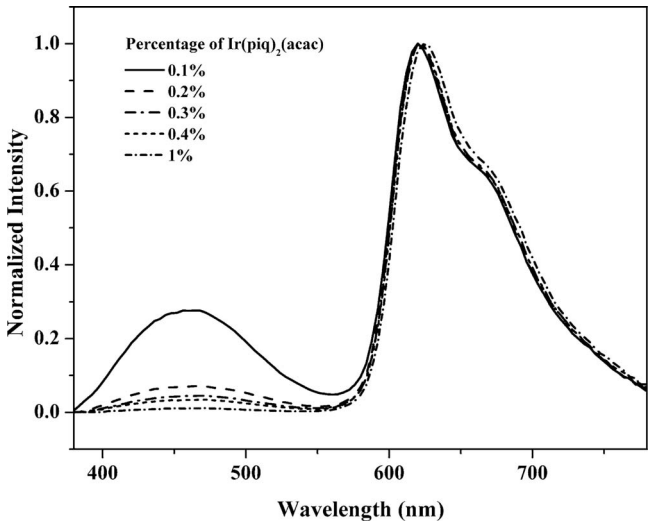

FIG. 10. EL spectra of OLEDs with configuration ITO/PEDOT/PVK-OXD7(30%)-Ir(piq)$_2$(acac)(x%)/CsF/Al. Data are shown for different values of x.

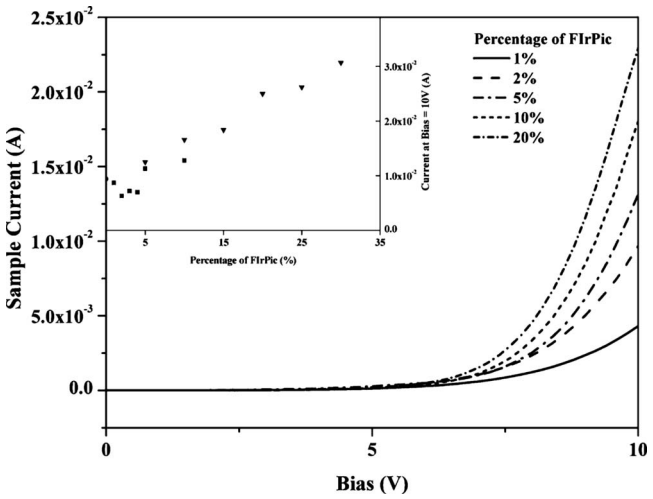

FIG. 11. Current vs bias characteristics for OLEDs with configuration ITO/PEDOT/PVK-OXD7(30%)-FIrpic(x%)-Ir(piq)$_2$(acac)(0.4%)/CsF/Al. Curves are shown for different concentrations of FIrpic. Inset shows the device current at an applied bias of 10 V vs the FIrpic concentration.

operating voltage of the OLED. This explains the rapidly decreasing luminous power efficiency with Ir(piq)$_2$(acac) concentration (Fig. 7).

Devices without FIrpic were also studied, i.e., OLEDs containing only the red dye. Figure 10 shows the normalized EL spectra for OLEDs with configuration ITO/PEDOT/PVK-OXD7(30%)-Ir(piq)$_2$(acac)(x%)/CsF/Al, in which x was varied from 0.1% to 1%. The shape of the main emission bands (peak at 630 nm together with a shoulder at about 670 nm) is unaffected over the concentration range investigated. However, a further broad emission, centered around 470 nm, is also evident. This is probably associated with PVK-OXD7 exciplex formation (Fig. 2) and indicates that the excitation process of the Ir(piq)$_2$(acac) molecules may not be as efficient as that of FIrpic. The maximum luminous efficiency and luminous power efficiency of the devices containing only the Ir(piq)$_2$(acac) dye were 3.2 cd A^{-1} and 1.3 lm W^{-1}, respectively. These were measured for a ITO/PEDOT/PVK-OXD7(30%)-Ir(piq)$_2$(acac) (0.4%)/CsF/Al OLED, at a current of 1 mA.

C. Effect of blue dye concentration

Figure 11 shows the current versus voltage characteristics for ITO/PEDOT/PVK-OXD7(30%)-FIrpic(x%)-Ir(piq)$_2$(acac)(0.4%)/CsF/Al OLEDs. The inset reveals the current (measured at an applied voltage of 10 V) dependence on the FIrpic concentration x for a larger number of devices; the data represented by the three different symbols refer to measurements made on different sets of samples. The overall trend is a gradual increase in the current with the FIrpic concentration. This contrasts with the effects of the addition of Ir(piq)$_2$(acac) molecules described in the last section and is consistent with the fact that the HOMO level of the FIrpic lies below that of the PVK host. The increase in the current with the blue dye concentration is probably associated with an additional current path provided by the hopping between FIrpic molecules. The effect of the different blue dye concentrations on the power efficiency of a white OLED is depicted in Fig. 12. An optimum efficiency is obtained for a FIrpic concentration of 3%–4%.

D. Two-layer devices

To elucidate further the excitation processes at work in our OLEDS, we have fabricated and studied OLEDs in which the blue and red phosphorescent dyes were contained in separate emitting layers. Two device configurations were investigated, in which either the blue-doped layer or the red-doped layer was adjacent to the ITO/PEDOT electrode. These devices were fabricated by spin-coating the first layer (PVK+OXD7+dye) onto a PEDOT-coated substrate, spin-coating the second layer, and then annealing the device. In some cases, the partly formed OLED was additionally annealed following the spin-coating of the first dye layer. However, subsequent electrical measurements revealed that this particular processing step did not make a significant differ-

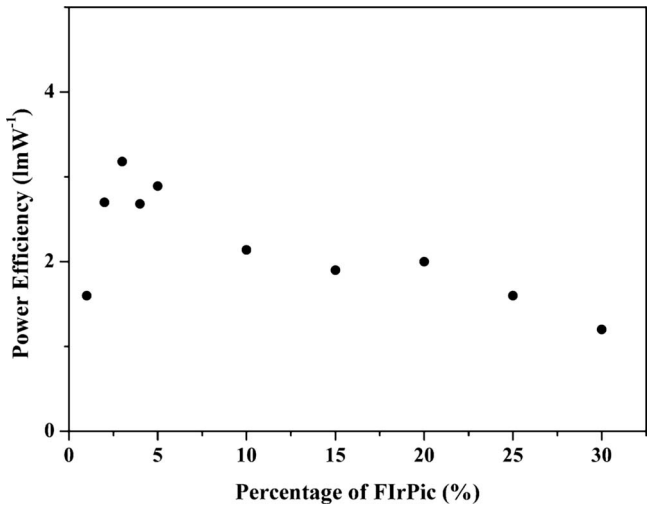

FIG. 12. Luminous power efficiency, measured at 1 mA, vs FIrpic concentration for OLEDs with configuration ITO/PEDOT/PVK-OXD7(30%)-FIrpic(x%)-Ir(piq)$_2$(acac)(0.4%)/CsF/Al.

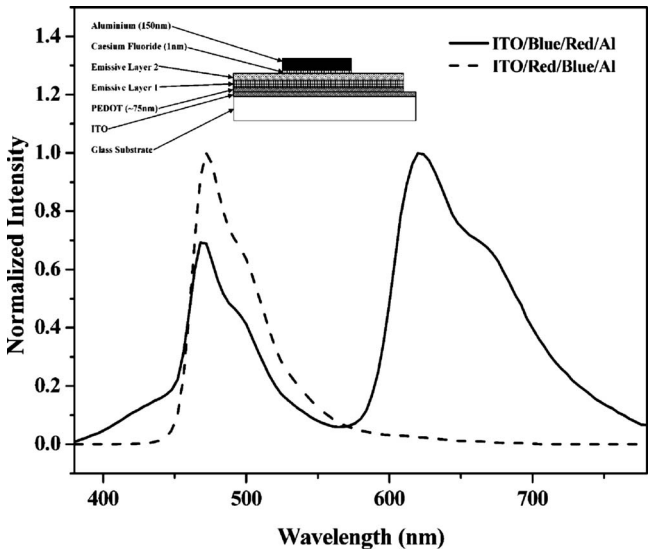

FIG. 13. Normalized EL spectra for dual emissive layer OLEDs with configurations ITO/PEDOT/PVK-OXD7(30%)-FIrpic(10%)/PVK-OXD7 (30%)-Ir(piq)$_2$(acac)(0.4%)/CsF/Al (depicted ITO/Blue/Red/Al) and ITO/PEDOT/PVK-OXD7(30%)-Ir(piq)$_2$(acac) (0.4%)/PVK-OXD7(30%)-FIrpic(10%)/CsF/Al (depicted ITO/Red/Blue/Al). The device structure is shown inset.

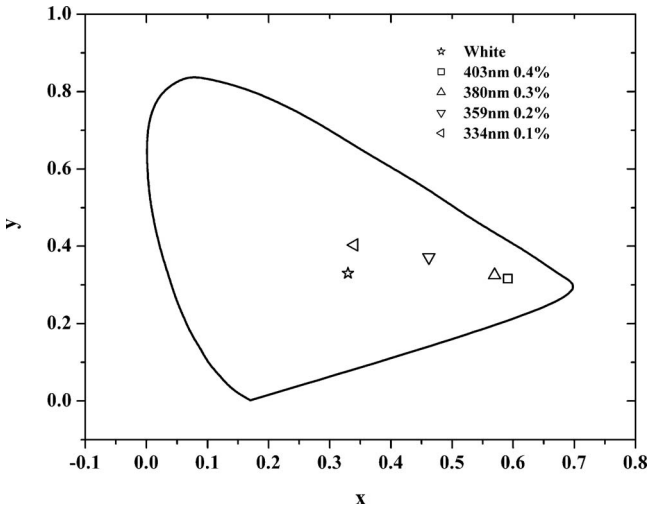

FIG. 14. CIE diagram showing coordinates for OLEDs with configuration ITO/PEDOT/PVK-OXD7(30%)-FIrpic(10%)-Ir(piq)$_2$(acac)(x%)/CsF/Al. Data points are for 330–400-nm-thick devices with different x values.

ence. The normalized EL spectra from the two types of dual-layer device are shown in Fig. 13, with the device configuration inset. Although both device configurations emit blue light, red emission is only achieved for OLEDs in which the red phosphorescent dye is adjacent to the to CsF/Al electrode. Interestingly, the fact that two different EL outputs were obtained for the two OLED configurations reveals that the second spin-coating step (using the same solvent as the first step) did not appreciably affect the underlying layer, i.e., the resulting multilayer structure is as depicted in the inset of Fig. 13, with little intermixing of the dyes.

The results shown in Fig. 13 confirm the suggestion above that the excitation mechanism of the red and blue dyes is different. The FIrpic is excited by direct energy transfer from the PVK host. Excitons formed in the PVK can transfer their energy directly to the FIrpic molecules, irrespective of whether these are present in the PVK layer adjacent to the anode or the cathode. However, the Ir(piq)$_2$(acac) red dye is only excited when it is doped into the PVK layer adjacent to the CsF/Al electrode. The process by which these dye molecules are excited is by hole trapping followed by capture of electrons. This mechanism is clearly hindered when the red dye is deposited onto the ITO/PEDOT anode as the supply of electrons will be limited. Emission from the PVK-OXD7 exciplex is also evident for the OLED in which the red dye is adjacent to the cathode. This EL is presumably emitted from the PVK-OXD7-Ir(piq)$_2$(acac) layer, as observed previously for single layer structures with no blue dye (Fig. 10). It should be noted that the efficiency of the dual-layer devices was significantly lower (<1 lm W^{-1}) than for the single emissive layer structure.

E. Device thickness

In Section III A, it was shown that the emission of our blue OLEDs became redshifted due to microcavity effects, as the device thickness was increased (Fig. 3). As the efficiency of the these structures decreased rapidly with increasing Ir(piq)$_2$(acac) concentration (Fig. 7), we have explored the possibility of making improved white OLEDs by simultaneously increasing the device thickness while reducing the concentration of Ir(piq)$_2$(acac). The results are summarized in Table II and the CIE diagram in Fig. 14. These devices are significantly thicker (330–400 nm) than those reported earlier in this paper (<200 nm). Figure 14 reveals that approximate white emission (0.34, 0.40) can be achieved by the addition of only 0.1% of Ir(piq)$_2$(acac) by increasing the thickness of the organic layers. Although the luminous efficiency of the OLEDs has increased over the values reported in Section III B [a maximum of 11 cd A^{-1} was measured for a 334 nm device containing only 0.1% Ir(piq)$_2$(acac)], the luminous power efficiency has decreased as a greater voltage has to be applied to the OLED in order to achieve the same brightness.

TABLE II. Optoelectronic properties of ITO/PEDOT/PVK-OXD7(30%)-FIrpic(10%)-Ir(piq)$_2$(acac)(x%)/CsF/Al OLEDs for different thickness of the active layer and different concentrations of Ir(piq)$_2$(acac). The film thickness was varied by changing the concentration of the solution used for spin-coating.

Weight concentration of Ir(piq)$_2$(acac) (%)	Total thickness of organic layers(nm)	Device turn-on voltage(V)	Brightness at 1 mA(cd m^{-2})	CIE coordinates at 1 mA(x,y)	Luminous efficiency at 1 mA(cd A^{-1})	Luminous power efficiency at 1 mA(lm W^{-1})
0.4	403	10.2	386	0.59,0.32	7.6	0.6
0.3	380	8.0	460	0.57,0.32	9.0	0.8
0.2	359	7.3	536	0.46,0.37	11.0	1.1
0.1	334	6.5	550	0.34,0.40	11.0	1.3

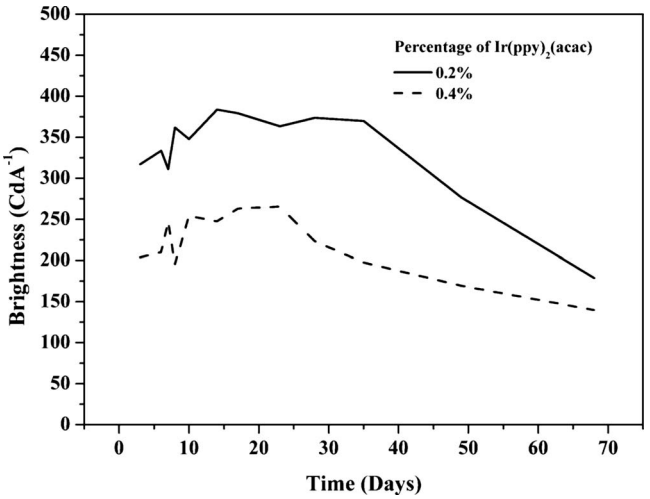

FIG. 15. Brightness vs storage time (in a desiccator) for OLEDs with configurations ITO/PEDOT/PVK-OXD7(30%)-FIrpic(10%)-Ir(piq)$_2$(acac) (x%)/CsF/Al. Full line x=0.2; dashed line x=0.4.

F. Lifetime

In a previous study we have reported on the increased stability that can be achieved with some blended-layer OLEDs.[7] We therefore have undertaken a preliminary investigation into the lifetime of the devices reported here. The blended-layer devices were kept in a desiccator (under vacuum) and periodically removed to monitor their EL behavior (measurements in air). Results for OLEDs with differing amounts of the red dye are shown in Fig. 15. Both devices exhibited the same trend in the brightness (measured at a forward current of 0.5 mA) versus time characteristics. Over the first three weeks there is an improvement in the output of the devices, which is then followed by a decline over the subsequent weeks. The latter is not unexpected, as the OLEDs were not encapsulated.

The main processes responsible for device degradation include:[28–34] oxidation of the emissive polymer film, possibly by extraction of oxygen atoms from the ITO anode or by the passage of electrons through the organic layer; formation of "hot spots," which undergo thermal runaway and lead to electrical short-circuits; a morphological change in the polymer film; changes in the mobility or injection of the charge carriers; reaction of the top electrode with water and/or oxygen; poor contact between the organic layer and the electrode(s), leading to dark areas in the image of the EL output; ion diffusion from the substrate; and electron trap formation. A device efficiency improvement over time is unusual. The organic layers in the OLED had all been annealed at 80 °C, prior to evaporation of the CsF and Al cathode. It would therefore seem unlikely that this layer would undergo further morphological changes while stored at room temperature. One explanation might be associated with the growth of an oxide layer beneath the Al cathode, which could lead to an improvement in the electron injection into the OLED, i.e., playing a similar role to the thin CsF layer. Such a process might be enhanced by oxygen atoms diffusing from the ITO anode. Notwithstanding the underlying physics, the relative stability of the unencapsulated blended-layer OLEDs augurs well for their future exploitation.

IV. CONCLUSIONS

We have investigated the electronic and optoelectronic behavior of white OLEDs based on blue (FIrpic) and red [Ir(piq)$_2$(acac)] phosphorescent dyes doped into the same layer of a PVK host. By studying systematically the current versus voltage and EL characteristics of various compositions of the blended layer, we have identified different excitation processes for the FIrpic and Ir(piq)$_2$(acac) molecules. The FIrpic molecules appear to be excited by direct transfer of the exciton energy from the PVK to the dye molecules, while the process of light emission from the Ir(piq)$_2$(acac) molecules involves carrier trapping. The efficiency of the devices can be tuned by incorporation of the electron transport compound OXD7 into the single layer blend and, to some extent, by varying the thickness of the organic film. Maximum luminous efficiencies and luminous power efficiencies of about 8 cd A^{-1} and 3 lm W^{-1} (CIE coordinates 0.35, 0.35) were measured for these blended-layer OLEDs. Although these values fall short of those currently quoted for white OLEDs, they have been obtained for a relatively simple device configuration, which should be relatively easy to manufacture.

ACKNOWLEDGMENTS

This work was partly supported by Durham County Council under the Science and Technology for Business and Enterprise Programme SP/717.

[1] *Organic Light-Emitting Materials and Devices*, edited by L. Zhang and H. Meng (Taylor & Francis, Boca Raton, 2007).
[2] B. W. D'Andrade and S. R. Forrest, Adv. Mater. **16**, 1585 (2004).
[3] B. C. Krummacher, V.-E. Choong, M. K. Mathai, S. A. Choulis, F. So, F. Jermann, T. Fielder, and M. Zachau, Appl. Phys. Lett. **88**, 113506 (2006).
[4] *Highly Efficient OLEDs with Phosphorescent Materials*, edited by H. Yersin (Wiley-VCH, Weinheim, 2008).
[5] S. Reineke, F. Lindner, G. Schwartz, N. Seidler, K. Walzer, B. Lüssem, and K. Leo, Nature (London) **459**, 234 (2009).
[6] J. H. Ahn, C. Wang, C. Pearson, M. R. Bryce, and M. C. Petty, Appl. Phys. Lett. **85**, 1283 (2004).
[7] J. H. Ahn, C. Wang, I. F. Perepichka, M. R. Bryce, and M. C. Petty, J. Mater. Chem. **17**, 2996 (2007).
[8] S. Tokito, T. Iijima, Y. Suzuri, H. Kita, T. Tsuzuki, and F. Sato, Appl. Phys. Lett. **83**, 569 (2003).
[9] G. Y. Park, J.-H. Seo, Y. K. Kim, Y. S. Kim, and Y. Ha, Jpn. J. Appl. Phys., Part 1 **46**, 2735 (2007).
[10] L. Qian, D. Bera, and P. H. Holloway, Appl. Phys. Lett. **90**, 103511 (2007).
[11] X. Jiang, R. A. Register, K. A. Killeen, M. E. Thompson, F. Pschenitzka, T. R. Hebner, and J. C. Sturm, J. Appl. Phys. **91**, 6717 (2002).
[12] K.-F. Shao, X.-J. Xu, G. Yu, Y.-Q. Liu, and L.-M. Yang, Chem. Lett. **35**, 404 (2006).
[13] T. Tsuboi, H. Murayama, S.-J. Yeh, M.-F. Wu, and C.-T. Chen, Opt. Mater. (Amsterdam, Neth.) **31**, 366 (2008).
[14] J. Lee, J.-I. Lee, K.-I. Song, S. J. Lee, and H. Y. Chu, Appl. Phys. Lett. **92**, 133304 (2008).
[15] P. E. Burrows, V. Khalfin, G. Gu, and S. R. Forrest, Appl. Phys. Lett. **73**, 435 (1998).
[16] V. Cimrová and D. Neher, J. Appl. Phys. **79**, 3299 (1996).
[17] I. D. Parker, J. Appl. Phys. **75**, 1656 (1994).
[18] A. J. Campbell, D. D. C. Bradley, and D. G. Lidzey, J. Appl. Phys. **82**, 6326 (1997).
[19] A. J. Campbell, M. S. Weaver, D. G. Lidzey, and D. D. C. Bradley, J. Appl. Phys. **84**, 6737 (1998).
[20] S. Karg, M. Meier, and W. Riess, J. Appl. Phys. **82**, 1951 (1997).
[21] M. Meier, S. Karg, and W. Riess, J. Appl. Phys. **82**, 1961 (1997).
[22] A. Rose, *Concepts in Photoconductivity and Allied Problems* (Robert E.

Krieger, New York, 1978).
[23]J. Lee, N. Chopra, S.-H. Eom, Y. Zheng, J. Xue, F. So, and J. Shi, Appl. Phys. Lett. **93**, 123306 (2008).
[24]V. I. Adamovich, S. R. Cordero, P. I. Djurovich, A. Tamayo, M. E. Thompson, B. W. D'Andrade, and S. R. Forrest, Org. Electron. **4**, 77 (2003).
[25]D. O'Brien, A. Bleyer, D. G. Lidzey, D. D. C. Bradley, and T. Tsutsui, J. Appl. Phys. **82**, 2662 (1997).
[26]X. H. Yang, F. Jaiser, S. Klinger, and D. Neher, Appl. Phys. Lett. **88**, 021107 (2006).
[27]J. Pina, J. Seixas de Melo, H. D. Burrows, A. P. Monkman, and S. Navaratnam, Chem. Phys. Lett. **400**, 441 (2004).
[28]J. C. Scott, J. H. Kaufman, P. J. Brock, R. DiPietro, J. Salem, and J. A. Goitia, J. Appl. Phys. **79**, 2745 (1996).
[29]I. D. Parker, Y. Cao, and C. Y. Yang, J. Appl. Phys. **85**, 2441 (1999).
[30]G. Y. Jung, A. Yates, I. D. W. Samuel, and M. C. Petty, Mater. Sci. Eng., C **14**, 1 (2001).
[31]H. Aziz and Z. D. Popovic, Appl. Phys. Lett. **80**, 2180 (2002).
[32]J. Lee, S. Sohn, H. J. Yun, and H. J. Shin, Appl. Phys. Lett. **93**, 133310 (2008).
[33]K. Fehse, R. Meerheim, K. Walzer, K. Leo, W. Lovenich, and A. Elschner, Appl. Phys. Lett. **93**, 083303 (2008).
[34]F. L. Wong, M. K. Fung, S. L. Tao, S. L. Lai, W. M. Tsang, K. H. Kong, W. M. Choy, C. S. Lee, and S. T. Lee, J. Appl. Phys. **104**, 014509 (2008).